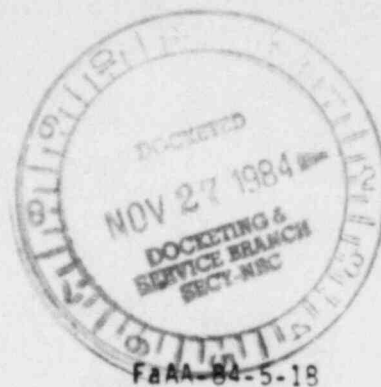


Lilco Docket p-36

50-322 OL A-36
10/1/84

**Failure
Analysis
Associates**

ENGINEERING AND METALLURGICAL CONSULTANTS
2225 EAST BAYSHORE ROAD, PO. BOX 51470
PALO ALTO, CALIFORNIA 94303-4151 TEL: 940-7042 FAX



7396/DOH:R03341A

THE INFLUENCE OF THERMAL DISTORTION ON THE
FATIGUE PERFORMANCE OF AF AND AE PISTON SKIRTS

Prepared by
Failure Analysis Associates
2225 E. Bayshore Road
Palo Alto, California 94303

Prepared for
TDI Diesel Generator Owners Group

NUCLEAR REGULATORY COMMISSION

Docket No. 50-322 Official Exh. No. # 36
In the matter of LILCO
June 1984
Staff _____ IDENTIFIED ☒
Applicant ☒ RECEIVED ☒
Intervenor _____ REJECTED _____
Conf'g Off'r _____
Contractor _____ DATE 10-1-84
Other _____ Witness _____
Reporter WRB

8412130316 841001
PDR ADOCK 05000322
G PDR

STATEMENT OF APPLICABILITY

This report addresses the structural adequacy of the Transamerica Delaval Inc. types AE and AF piston skirts supplied for use in R-4 series diesel engines. The modified type AF skirt was originally installed in the engines at Shoreham Nuclear Power Station, Grand Gulf Nuclear Station, and San Onofre Nuclear Generating Station. These skirts have been replaced at Shoreham and Grand Gulf by type AE skirts. Type AE skirts have also been installed at Comanche Peak Steam Electric Station. Evaluation of the type AF skirts at San Onofre will be reported separately.

EXECUTIVE SUMMARY

This report addresses the influence of thermal distortion of the piston crown on the structural integrity of the Transamerica Delaval Inc. (TDI) types AE and AF piston skirts. This report is an extension of earlier work* which provided the results of experiments and finite element analyses on these skirts under isothermal conditions. This report was prepared on behalf of the TDI Diesel Generator Owners Group as one of a series of reports on generic components of those diesel engines in nuclear installations -- the generically termed Phase I components.

The cyclic stresses, and therefore the fatigue performance, of the piston skirts is influenced by load transfer between the skirt and the crown on the two concentric rings over which the crown and skirt can contact one another. This load transfer is influenced by thermal distortion of the crown and the initial size of the gap between the crown and skirt. The influence of thermal distortion and initial gap on cyclic stress levels and the possibility of lift-off of the crown from the skirt were estimated by combining the results of isothermal finite element stress analysis with a crown/skirt interaction model. The crown/skirt interaction model treats the crown and the skirt as springs whose stiffnesses were estimated by finite element techniques. Thermal distortion is included as a thermally-induced displacement that is calculated by finite elements using a steady-state temperature field in the piston assembly based on experimental measurements. Predicted and observed gap closure pressures and load transfers between the contact rings agreed well with one another.

Cyclic stresses under isothermal and steady-state operation were calculated by use of the crown/skirt model for a variety of initial gap sizes. The influence of lift-off was included in cases where it was predicted to occur.

* "Investigation of Types AE and AF Piston Skirts," Report prepared by Failure Analysis Associates for Transamerica Delaval Inc. Diesel Generator Owners Group, Report No. FaAA-84-2-14, Palo Alto, California, May 1984.

Crack initiation and propagation analyses were then performed by procedures followed in earlier isothermal analyses.

The conclusions obtained earlier regarding cracking of the AE and AF skirts were unchanged, but now the arrested crack depths predicted for the AF are in better agreement with field observations. Overall, the earlier conclusions regarding the integrity of the AE and AF skirts are also unchanged. These conclusions are that cracks may initiate but will not propagate in the AE, and that cracks will initiate and may propagate in the AF. However, any cracks in the AF are predicted to arrest at depths less than 0.5 inch, which is comparable to field observations of cracking reported earlier.

TABLE OF CONTENTS

<u>Section</u>	<u>Page</u>
• STATEMENT OF APPLICABILITY.....	i
EXECUTIVE SUMMARY.....	ii
1.0 INTRODUCTION.....	1-1
Section 1 References.....	1-2
2.0 FINITE ELEMENT ANALYSIS.....	2-1
2.1 Load Considerations.....	2-1
2.2 Stress Analysis.....	2-3
2.3 Stiffness Analysis.....	2-4
2.3.1 Skirts.....	2-4
2.3.2 Crown.....	2-5
2.4 Crown/Skirt Interaction.....	2-8
Section 2 References.....	2-9
3.0 CROWN/SKIRT INTERACTION MODEL.....	3-1
3.1 Review of Experimental Observations.....	3-1
3.1.1 Piston Assembly.....	3-1
3.1.2 Stud Attachment Loads and Stiffnesses.....	3-2
3.2 Crown/Skirt Interaction Model.....	3-3
3.2.1 Power Stroke.....	3-4
3.2.2 Exhaust Stroke.....	3-7
3.3 Comparison with Experimental Observations.....	3-10
Section 3 References.....	3-11
4.0 FATIGUE AND FRACTURE ANALYSIS.....	4-1
4.1 Cyclic Stresses.....	4-1
4.2 Fatigue Crack Initiation Analysis.....	4-2
4.3 Fatigue Crack Growth Analysis.....	4-3
Section 4 References.....	4-5
5.0 CONCLUSIONS.....	5-1
APPENDIX A: COMPONENT TASK DESCRIPTION.....	A-1

1.0 INTRODUCTION

The purpose of this report is to address the influence of thermal distortion on the fatigue performance of Transamerica Delaval Inc. types AE and AF piston skirts. This report is an extension of earlier work [1-1] which provided the results of experiments and finite element analyses on these skirts under isothermal conditions. This report draws heavily on Reference 1-1.

The largest stresses in absolute value in the piston skirt result from firing pressure. The peak firing pressure occurs when the piston is close to its top dead center (TDC) position on the firing stroke. The pressure force on the crown is transmitted between the crown and the top of the skirt in part on the ring that coincides with the stud attachment bolt circle. This ring is referred to as the inner ring. Load transfer between the crown and skirt can also occur on an outer ring. The crown is assembled to the skirt to provide a gap between the crown and skirt at the outer ring of 0.007 to 0.011 inch. When pressure is applied to the top of the crown, the crown and skirt deform, thereby tending to close the gap. Load transfer between the crown and skirt is altered when the gap closes, thereby affecting the peak stresses in the skirt.

Once the engine reaches steady-state operating conditions, large temperature gradients are present in the crown. These temperature gradients distort the crown, thereby changing the gap. Such changes also influence load transfer and stresses in the skirt. If thermal distortion of the crown is sufficiently large, it is conceivable that the resulting forces, when combined with the inertia forces at TDC of the exhaust stroke, will exceed the stud preload. This would allow the crown to lift off of the skirt on the inner contact ring, which would unload a portion of the contact surface, thereby altering the stresses during this part of the cycle.

The influence of thermal distortion and possible crown lift-off are addressed by combining the results of finite element analyses and experimental observations reported in Reference 1-1 with additional finite element analyses, experimental observations of steady-state crown temperatures and a

model of the interaction of the crown and the skirt. Cyclic stresses in the stud boss region of the AE and AF skirts for various gap sizes and for steady-state temperature distribution and isothermal conditions are obtained. These stresses are then used in fatigue and fracture mechanics analyses of crack initiation and growth to provide predictions of crack behavior in these skirts.

Section 1 References

- 1-1. "Investigation of Types AF and AE Piston Skirts," Report prepared by Failure Analysis Associates for Transamerica Delaval Inc. Diesel Generator Owners Group, Report No. FaAA-R4-2-14, Palo Alto, California, May 1984.

2.0 FINITE ELEMENT ANALYSIS

The results of finite element analyses of stresses in AE and AF piston skirts are presented in this section along with analyses of thermal distortion of the crown. The skirt analyses were performed using the same global and local finite element models that were previously constructed for the isothermal analysis reported in Reference 2-1. Spring constants of the skirts and crown were also evaluated by finite elements. These stiffnesses are used in the crown/skirt interaction model presented in Section 3 to provide estimates of cyclic stresses for use in the fatigue and fracture analysis of Section 4.

2.1 Load Considerations

Three loads were assumed to be acting on the piston: gas pressure, reciprocating inertia, and friction. In addition, since the piston is a two-piece design, initial internal load is associated with the bolt preload. As part of the analysis of the crankshaft of these same engines [2-2], a table of gas pressure, accelerations, and friction was developed that provided values for every ten degrees of rotation of the crankshaft. This covered rotation from 0° to 720° thereby encompassing the entire four-cycle combustion process. The combined loading was found to be highest at top dead center during the power stroke. At this point, only pressure and inertia are acting on the piston since the velocity (and therefore friction) is essentially zero. A peak firing pressure of 1670 psig [2-2] was assumed to be acting when the piston is at top dead center.

A value of 379,000 pounds was obtained for the pressure load from the peak firing pressure and cylinder bore. At top dead center of the power stroke, the pressure load is somewhat offset by the inertia load, which is exerted by the crown on top of the skirt. The piston acceleration at top center was found from the crankshaft analysis to be 26.1×10^3 in/sec². The crown weighs 144 pounds. Therefore, the inertia force is $144 \times 26.1 \times 10^3 / 386.4 = 9727$ pounds. Subtracting this from the pressure force provides the maximum net force on the top of the skirt, 369,300 pounds. This corresponds to an effective pressure of 1527 psig.

The other extreme of the stress cycle in the skirt occurs at top dead center of the exhaust stroke, at which time a tensile load equal to the inertia force of the crown is applied at the top of the skirt. If lift-off between the crown and skirt does not occur, then the peak stress due to inertia can be obtained from the peak stress due to firing pressure by multiplying the peak pressure stress by the ratio of the inertia force to the peak pressure force (and changing the sign to account for the different direction of the loads). If crown/skirt lift-off does occur, then the load path of the inertia force at top dead center of the exhaust stroke is different than the path at top dead center of the power stroke. Under such conditions, the peak stresses during exhaust must be evaluated by a separate analysis, rather than by ratioing the power stroke results.

The following four sets of boundary conditions on the top of the skirt were considered for each skirt design:

1. Crown mounted on the top of the skirt with a frictionless interface at the inner contact ring. Pressure of 1627 psig is applied to the top of the crown, and the crown and skirt are allowed to deform without interfering with each other at the outer loading ring.
2. Uniform vertical displacement on the inner crown/skirt contact ring of a magnitude to react the loading corresponding to 1627 psig effective pressure on the crown.
3. Uniform vertical displacement on the outer crown/skirt contact ring of a magnitude to react the load corresponding to 1627 psig effective pressure on the crown.
4. A stud load applied on the stud washer landing area and reacting on the outer loading ring which is constrained to have a uniform vertical displacement.

Of these four cases, Case 1 provides the most realistic estimate of maximum stresses in the isothermal skirt in the absence of gap closure and also provides checks on the crown/skirt interaction model. This loading condition was the only one considered in Reference 2-1. Cases 2 and 3 provide estimates of the skirt spring constants that are required for the crown/skirt interaction model discussed in Section 3. Comparison of Case 1 with Cases 2

and 3 provides information on the suitability of simplified boundary conditions at the top of the skirt. Case 4 provides stress levels at top dead center of the exhaust stroke appropriate for crown/skirt lift-off. A rigid wrist pin was assumed in Cases 1-3; no wrist pin was utilized for Case 4. All finite element runs on the skirt models were performed for uniform temperature.

2.2 Stress Analysis

Stresses and displacements for the four loads and boundary conditions discussed in Section 2.1 were calculated for the AE and AF skirts using the ANSYS finite element computer program. Details of the models employed are provided in Reference 2-1. Spring constants were evaluated from the global models, and stresses were obtained by combining the global and local models as described in Reference 2-1. The stress results are summarized in Table 2-1. The third algebraic minimum principal stress (σ_{III}) is provided for firing pressure results, and the maximum principal stress (σ_I) is provided for the lift-off condition. These stresses are pertinent to the fatigue analysis discussed in Section 4. The equivalent stress, σ_e , is also included in Table 2-1.

The results of Table 2-1 show that the AF piston skirt generally has considerably larger stresses than the AE. This is especially true for the two conditions of primary interest -- pressurized crown and lift-off as calculated from the local models. The appreciable increase in σ_{max} when lift-off occurs is apparent from the results in Table 2-1. The relatively small difference between the stresses for the AE and AF skirts for uniform displacement on the inner contact ring indicates that this idealized boundary condition does not point out the large stress difference in these two skirts that results from the more realistic boundary conditions provided by placing the crown on the skirt. Fairly large stress differences between the two skirt designs were observed to be present in strain gage measurements and are indicated by differences in cracking behavior under service conditions -- as reported in Reference 2-1. The results of Table 2-1 also show that the peak stresses in the stud boss region are much more influenced by loading on the inner contact ring, being virtually zero for loading only on the outer contact ring.

2.3 Stiffness Analysis

The results of finite element analyses of crown and skirt stiffnesses are presented in this section. These results are used in the crown/skirt interaction model described in Section 3.

2.3.1 Skirts

The relative displacements of the inner and outer contact rings between the crown and skirt control gap closure and the load split between the inner and outer contact rings. These relative displacements can be expressed in terms of spring constants. The values of the spring constants for the AE and AF skirts were obtained from the finite element calculations performed to obtain the stresses discussed in Section 2.2. The following spring constants are required:

stiffness of skirt at inner ring due to loading at inner ring, $k_i = F_i / \delta_i$;
stiffness of skirt at outer ring due to loading at inner ring, $k_{io} = F_i / \delta_o$;
stiffness of skirt at outer ring due to loading at outer ring, $k_o = F_o / \delta_o$;
stiffness of skirt at inner ring due to loading at outer ring, $k_{oi} = F_o / \delta_i$.

As discussed in Section 3, the reciprocity relation of linear elasticity requires that $k_{io} = k_{oi}$.

These stiffnesses were evaluated as part of the finite element stress analysis. The constants k_o and k_i are directly obtainable from the uniform displacement finite element runs. The evaluation of k_{oi} is subject to some uncertainty in the present case, because the non-loaded contact ring does not remain planar when the loaded contact ring is subjected to uniform vertical displacement. Hence, a uniform displacement of the non-loaded ring is not clearly defined. However, k_{oi} can be more clearly defined when displacements in the complete crown/skirt model are considered. This is discussed more fully in Section 2.4. Fortunately, the precise value of k_{oi} is not required, because this spring constant does not have a strong influence on the end results. Table 2-2 summarizes the calculated spring constants for the two skirt designs.

The vertical displacement on the top of the skirt along the stud bolt circle was evaluated as part of the finite element analysis of stresses due to stud loads under lift-off conditions. These displacements are relevant to crown lift-off, and are presented in Figure 2-1 for both the AE and AF skirts. A stud load of 6,600 pounds was used. As discussed in Section 3.1.2, this value is based on experimental measurements. A strong angular variation of skirt displacement is seen in Figure 2-1, which is especially marked for the AF skirt. The displacement is smallest over the wrist pin, as expected.

2.3.2 Crown

The crown is fabricated from cast steel and mounts on the top of the skirt. A 0.007-0.011 inch gap is present at the outer load ring at assembly. The crown enters into the analysis in two ways; for isothermal conditions, the pressure load applied to the top of the crown is transmitted through the crown to the top of the skirt in a manner which corresponds to neither a uniform displacement nor uniform loading boundary condition on the skirt, and thermal distortion of the crown due to non-uniform temperatures during engine operation influences the proportion of the pressure load that is transmitted across each of the loading rings.

Two separate finite element models of the crown were constructed. One was for placing on top of the skirt and is described in Reference 2-1. This model was needed only to represent the circumferential variation of the crown/skirt interfacial pressure, and was relatively coarse.

The other crown model was for evaluation of thermal distortion of the crown and stiffnesses of the crown due to pressure on the top and loading on the outer contact ring. This model must accurately predict the crown displacement at the outer ring relative to the inner ring, and, thus, was constructed with a much finer mesh. Figure 2-2 shows the axisymmetric model that was composed of 327 elements and 425 nodes. An axisymmetric bilinear displacement element was utilized for this refined crown model which was run using the MARC analysis program.

The vertical displacement of the outer contact ring relative to the inner contact ring when the crown is subjected to service conditions is of interest in evaluating the response of the crown and skirt to pressure and temperature loadings. The finite element model shown in Figure 2-2 was used for the calculations of crown deformation for various service loads. The inner ring of the crown model was assumed to be supported and the displacement of the outer ring was calculated for three conditions: (i) uniform pressure on top of the crown; (ii) axially oriented load around the circumference of the outer ring; and (iii) crown subjected to steady-state temperatures corresponding to engine operation.

The stiffness of the crown when subjected to pressure and outer ring loading was found by dividing the total load by the corresponding deflection of the outer contact ring. The following results were obtained:

Pressure stiffness

$$k_{c(p)} = pA/\delta = 47.4 \text{ kips/mil}$$

Outer ring loading stiffness

$$k_{c(F)} = F/\delta = 16.4 \text{ kips/mil}$$

p = pressure,

A = bore area,

F = outer contact ring load, and

δ = corresponding displacement of outer contact ring relative to inner ring.

The vertical deflection of the outer ring relative to the inner ring at steady-state operating conditions is also of interest. This parameter is denoted as δ_T , and its calculation requires information on the steady-state temperature distribution in the crown and skirt. In order to gain a better understanding of the crown temperatures under steady-state operating conditions, the results of peak temperature measurements as a function of position in the crown were supplied by TDI [2-3]. The measurements were made with "templugs," which were inserted into holes drilled in the crown and provided a passive measure of the maximum temperature to which the plug was subjected. As reported by TDI, the measurements were made in an R-4 engine at 450 RPM

with a BMEP of 213 psig, and closely follow the running conditions at Shoreham. The peak crown temperature measurements reported by TDI are shown in Figure 2-3. Note that the temperatures on the bottom of the crown are nearly constant and equal to about 200°F. This suggests that the piston skirt is nearly isothermal under steady-state operating conditions, which implies that thermal stresses in the skirt are small.

Independent calculations of operating temperature in the piston assembly were performed by Failure Analysis Associates. The transient radiative and convective heat transfer analysis utilized reasonable values for coolant temperatures, and convective heat transfer coefficients, and combustion gas temperatures determined from the indicator diagram data from Reference 2-1. Key features of the calculated temperature field, including peak temperature and temperature gradient through the central portion of the crown, were in agreement with the TDI measurements of temperature.

The temperatures at various positions on the surface of the crown shown in Figure 2-3 were used to estimate the steady-state operating temperatures everywhere on the crown boundary. These boundary temperatures then served as boundary conditions for an axisymmetric steady-state heat conduction problem. The finite element model shown in Figure 2-2 was used for numerical generation of the steady-state temperature distribution throughout the crown. This temperature field was then used for finite element calculation of thermally-induced displacements in the crown. This provided the following result for the (downward) movement of the outer ring relative to the inner ring under steady-state engine operating conditions:

$$\delta_T = 0.0106 \text{ inch}$$

This result is used in Section 3 to obtain estimates of the influence of thermal distortion on stresses in the skirt and possible lift-off of the crown from the skirt.

2.4 Crown/Skirt Interaction

Information on the interaction of the crown and skirt under isothermal conditions was provided in Reference 2-1 by experimental and finite element analyses that included the crown mounted on the skirt. The finite element results are briefly reviewed in this section. Figures 2-4 and 2-5, which are drawn directly from Reference 2-1, summarize the finite element results relevant to crown/skirt interaction. These figures show that there is considerable angular variation of vertical displacement in both the crown and the skirt in both the inner and outer rings. Hence, the contact rings do not remain planar, and uniform displacement of the contact rings does not provide an accurate representation of the boundary conditions on the top of the skirt. However, these figures show that the gap between the outer rings of the skirt and crown is virtually independent of angular position. This is evident by the flatness of the dashed line in these figures, which is the difference between the vertical displacement on the outer ring of the crown and skirt ($\delta_{co} - \delta_{so}$). The uniformity of the gap around the circumference of the pressurized crown/skirt means that gap closure will occur uniformly around the circumference -- despite the fact that the contact rings do not remain planar. This observation is consistent with the deduction from the experimental results reported in Reference 2-1 that the gap closes nearly simultaneously at all angular positions on the outer ring.

The stiffness of the crown when attached to the skirt and subjected to pressure [$k_c(p)$] and the value of k_{i0} can be estimated from the results presented in Figures 2-4 and 2-5. The value of the crown stiffness is given by the expression

$$k_c(p) = \frac{F}{\delta_{co} - \delta_{ci}} \quad (2-1)$$

The value of k_{i0} is given by the expression

$$k_{i0} = \left[\frac{1}{k_i} - \frac{\delta_{si} - \delta_{so}}{F} \right]^{-1} \quad (2-2)$$

where F = total applied force,

δ_{co} = vertical displacement of outer ring of crown,

δ_{ci} = vertical displacement of inner ring of crown,

δ_{so} = vertical displacement of outer ring of skirt,

δ_{si} = vertical displacement of inner ring of skirt, and

k_i = skirt stiffness at inner contact ring.

The value of k_i reported in Section 2.3.2 was used for the calculation of k_{io} . Table 2-3 summarizes the results of these stiffnesses. The value of $k_c(p)$ agrees well with the value of 47.4 kips/mil determined by finite element analysis of a stand-alone crown, as reported in Section 2.3.2. The slight difference in the values is due to the different degrees of model refinement. The values of k_{io} shown in Table 2-3 show a wide degree of variability in spite of a relatively constant value of the relative displacement. Fortunately, an accurate value of k_{io} is not required, because this relatively large stiffness plays a secondary role in the crown/skirt interaction -- the interaction being dominated by the smaller stiffnesses k_i , $k_c(p)$, and $k_c(F)$. A nominal value of 500 kips/mil was selected and is the value included in Table 2-2.

Section 2 References

- 2-1 "Investigation of Types AF and AE Piston Skirts," Report prepared by Failure Analysis Associates for Transamerica Delaval Inc. Diesel Generator Owners Group, Report No. FaAA-84-2-14, Palo Alto, California, May 1984.
- 2-2 "Emergency Diesel Generator Crankshaft Failure Investigation," Failure Analysis Associates Report No. FaAA-83-10-2, Palo Alto, California, October 1983.
- 2-3 Private communication from Al Fleischer, Transamerica Delaval Inc. to David Harris, Failure Analysis Associates, 6 January 1984.

Table 2-1

MAXIMUM PRINCIPAL AND EQUIVALENT STRESSES IN STUD BOSS REGION
 AS EVALUATED BY FINITE ELEMENTS FOR VARIOUS BOUNDARY
 CONDITIONS FOR THE AE AND AF PISTON SKIRTS
 (all stresses in ksi)

	Loading Condition	AE		AF	
		Global	Local	Global	Local
PRINCIPAL	Pressurized crown, σ_{III}	-42.7	-68.1	-41.4	-92.2
	Inner ring, unif. displ., σ_{III}	-28.5	-43.4	-29.4	-47.7
	Outer ring, unif. displ., σ_{III}	-5.71	-3.29	-2.22	-4.20
	Lift-off, $\sigma_I = q_{max}$	4.45	7.32	5.24	17.8
	No lift-off, $q_{max}^{(1)}$	--	1.77	--	2.40
EFFECTIVE	Pressurized crown	38.2	61.3	42.8	79.9
	Inner ring, unif. displ.	24.8	39.1	29.4	43.1
	Outer ring, unif. displ.	9.8	4.7	3.6	3.6
	Lift-off	3.88	6.78	5.55	19.8

(1) Equals $-(9727/369,300) \times (\sigma_{III} \text{ for pressurized crown})$.

Table 2-2
SUMMARY OF SKIRT STIFFNESSES FROM
FINITE ELEMENT ANALYSES
 (all values in kips/mil = millions of pounds/inch)

	AE	AF
k_i	81.2	70.5
k_o	95.3	94.2
$k_{io} = k_{oi}$	~500	~500

Table 2-3
STIFFNESSES EVALUATED FROM FULL CROWN/SKIRT
FINITE ELEMENT MODELS

		AE	AF
$\delta_{st} - \delta_{so}$, mils	ave	3.8	4.7
	max	4.1	5.0
	min	3.6	4.6
k_{io} , kips/mil	ave	493	686
	max	824	1547
	min	389	558
$\delta_{co} - \delta_{ci}$, mils	ave	6.4	7.0
	max	6.8	7.6
	min	5.6	6.4
$k_c(p)$, kips/mil	ave	52	53
	max	66	58
	min	54	49

$F = pA = 369$ kips

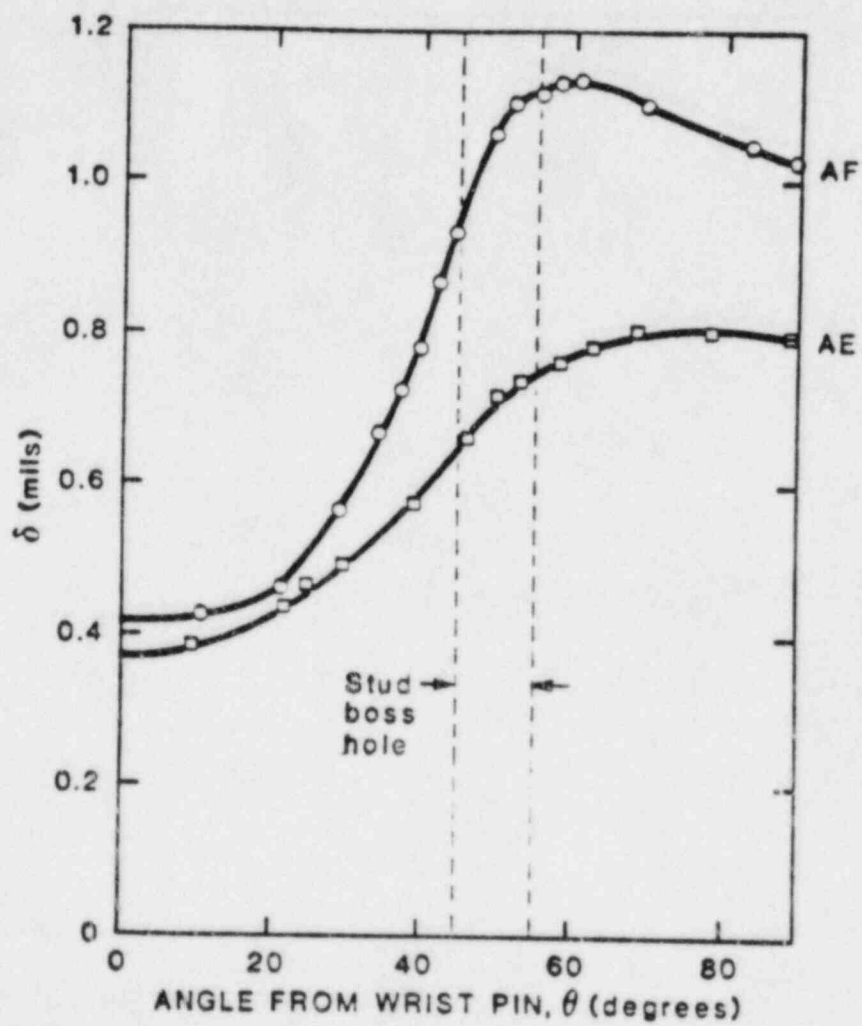


Figure 2-1. Vertical displacement of skirt at center row of nodes in inner contact ring for 6,600 lb. load applied at washer landing area.

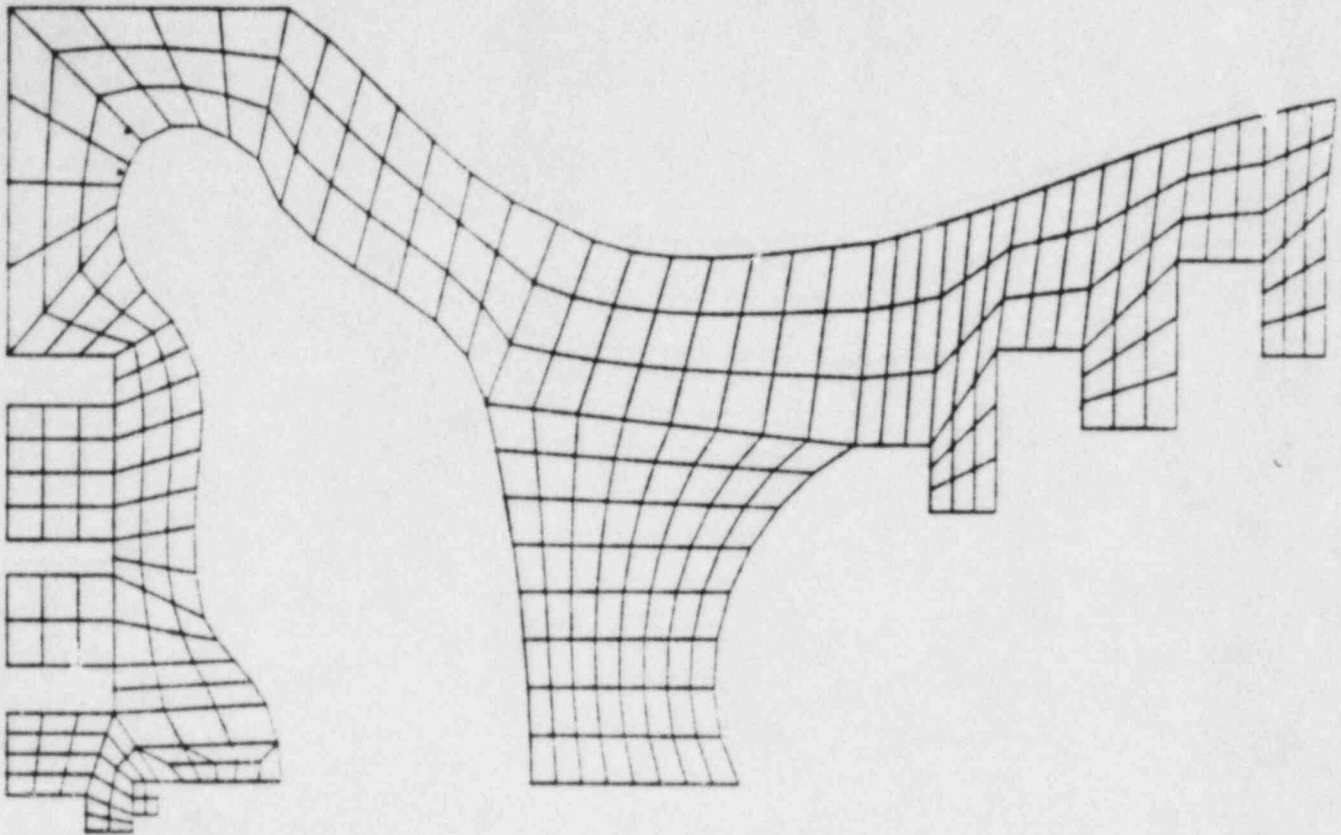


Figure 2-2. Finite element mesh of axisymmetric crown for evaluation of crown thermal distortion and spring constants.

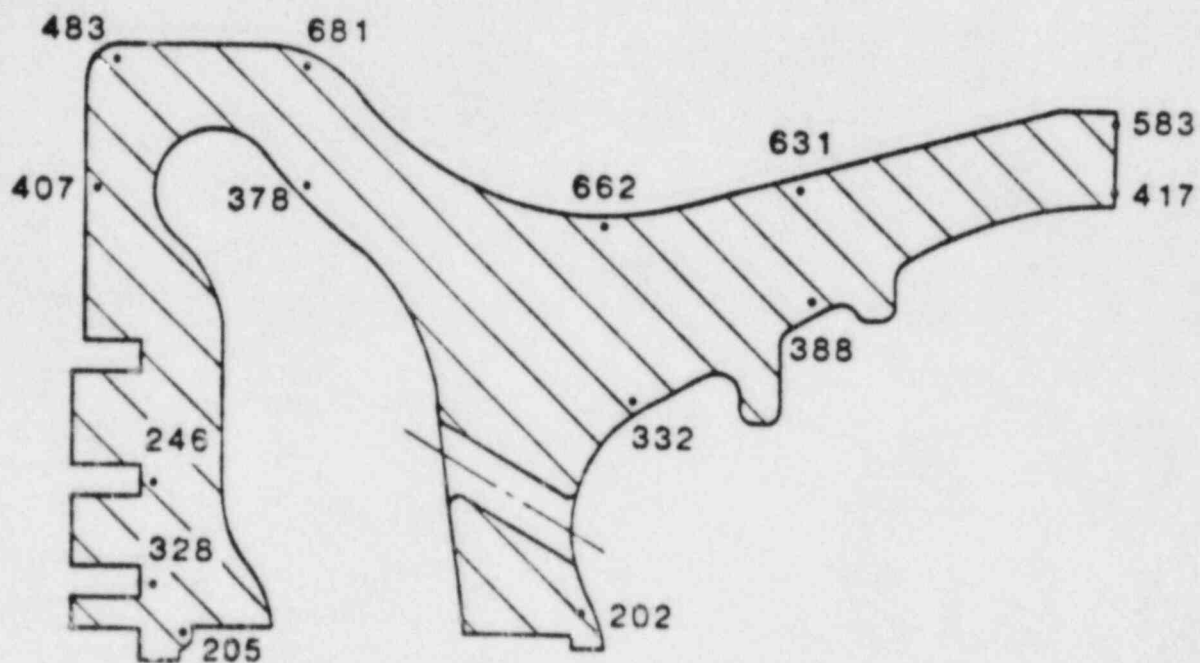


Figure 2-3. Results of templog measurements of peak temperature as a function of position on crown (supplied by TDI).

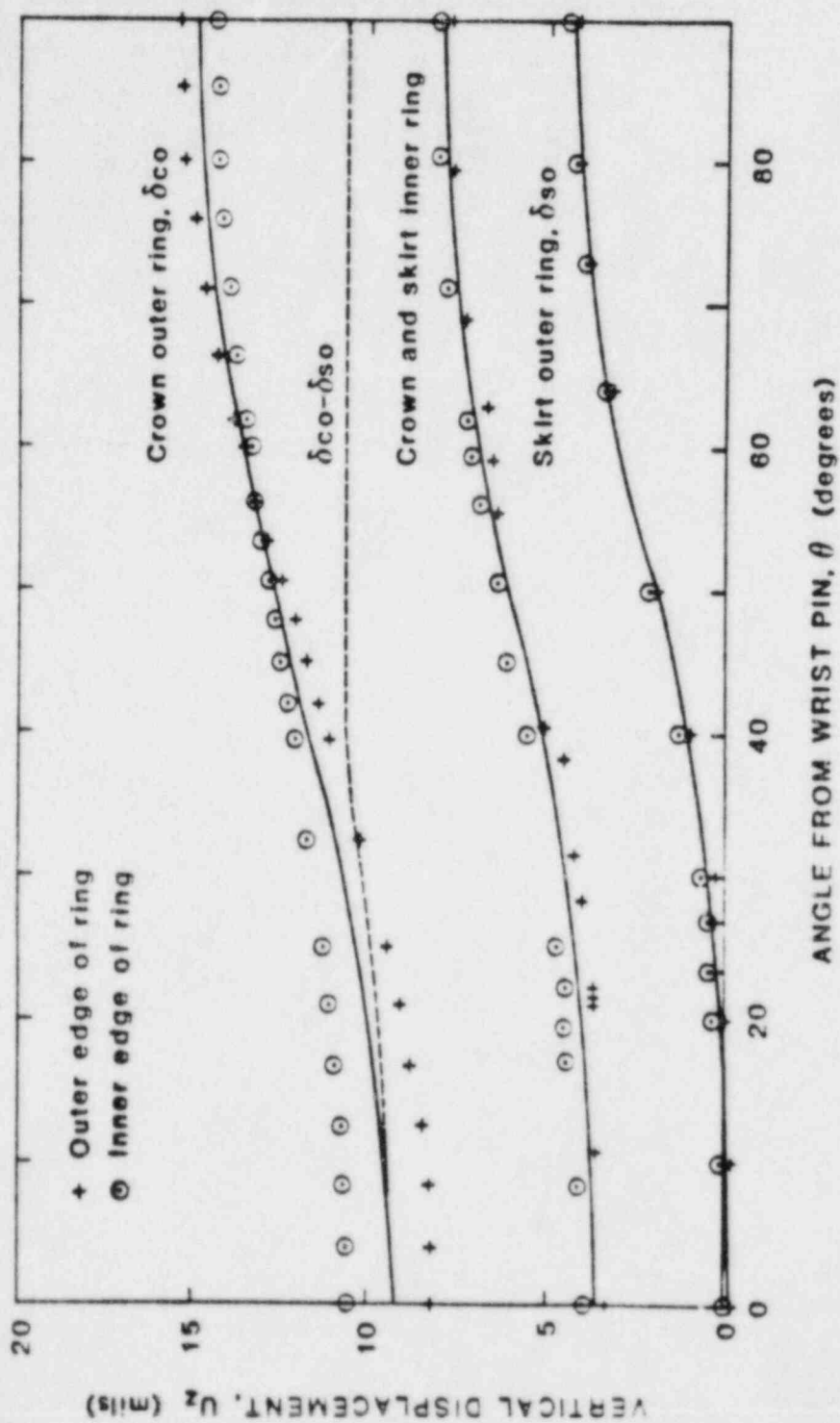


Figure 2-4. Computed crown and skirt vertical displacements on inner and outer rings as a function of angular displacement for an AE crown/skirt [2-1].

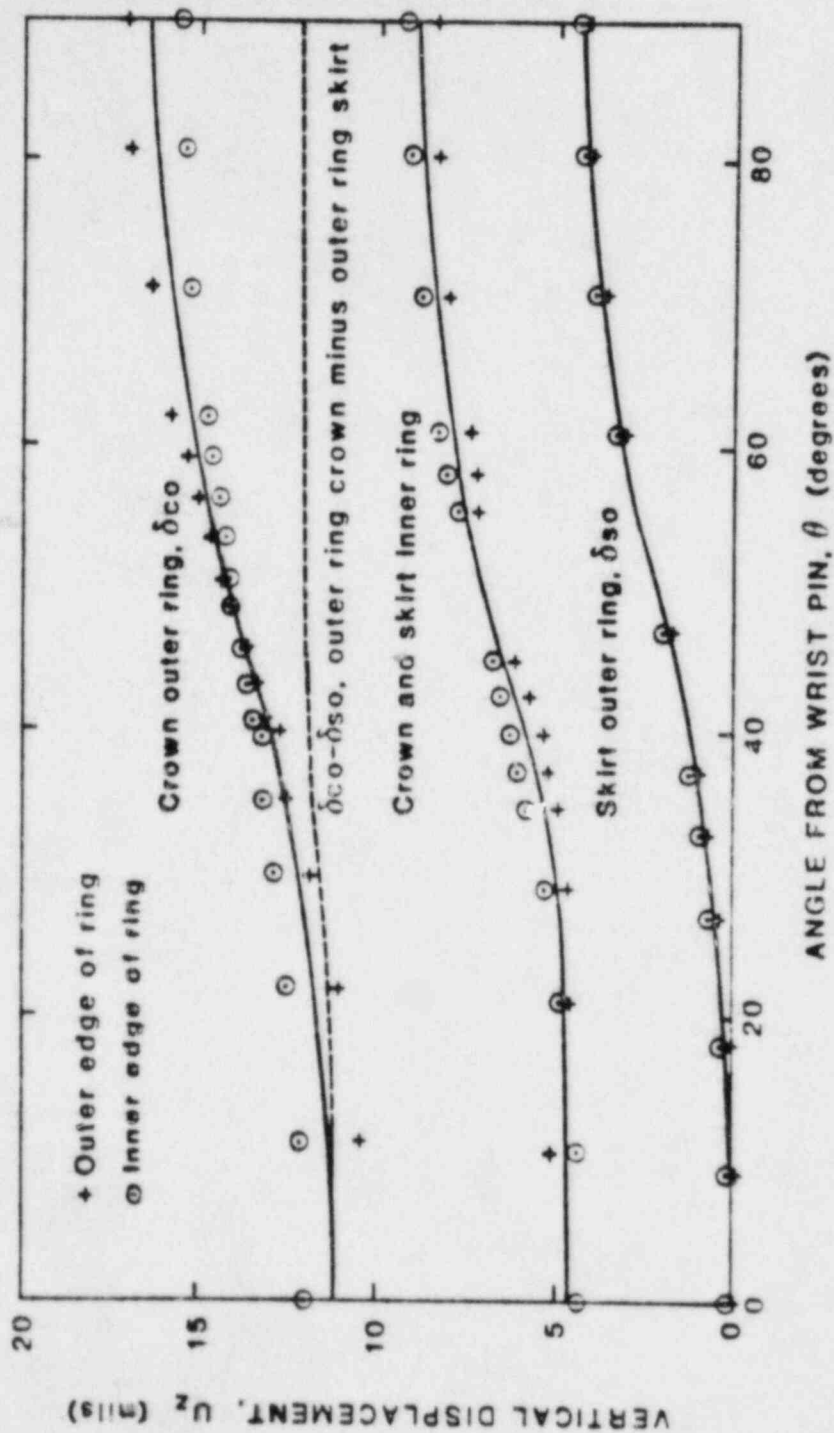


Figure 2-5. Computed crown and skirt vertical displacements on inner and outer rings as a function of angular position for an AF crown/skirt [2-1].

3.0 CROWN/SKIRT INTERACTION MODEL

A crown/skirt interaction model that includes the influence of thermal distortion of the crown on the load split between the contact rings and the possibility of lift-off between the crown and skirt is described in this section. Such effects are important because of their influence on cyclic stresses in the stud boss region under isothermal and steady-state operating conditions.

3.1 Review of Experimental Observations

A review of the experimental observations under isothermal conditions reported in earlier work [3-1] on the AE and AF skirts is provided along with some new closely related results.

3.1.1 Piston Assembly

The results of strain gage measurements at numerous locations on AE and AF pistons with hydrostatic pressure applied to the crown indicated that the gap closed nearly simultaneously around the circumference of the piston. The pressure at which the gap closed (under isothermal conditions) is denoted as p^* . The observation of simultaneous gap closure around the piston circumference is consistent with the finite element results presented in Figures 2-4 and 2-5 in which the gap (difference in displacement) is nearly independent of angular location in spite of the appreciable angular variation of the individual displacements. Once the gap is closed, some load is transmitted to the outer contact ring, thereby reducing the stress in the stud boss region below what it would be in the absence of gap closure.* The ratio of peak stud boss stresses with and without gap closure is of interest, because such stress reductions have an important influence on the value of cyclic stresses in this critical region. Additionally, experimental observations of stress reduction and gap closure provide results that are suitable for comparison with predic-

* The finite element results of Table 2-1 show that loading on the outer ring produces only minimal stresses in the stud boss region.

tions made by use of the crown/skirt model. Table 3-1 summarizes the experimental results of current interest.

3.1.2. Stud Attachment Loads and Stiffnesses

* The amount of preload on the studs that attach the crown to the skirt must be known to determine the possibility of crown lift-off, as discussed in Section 3. The stiffness of the belleville washer stack is also required. The values of these parameters were measured experimentally, and the results will be reported here.

Two foil strain gages were mounted on the central portion of a crown attachment stud, and the strain produced by attaching a crown to a modified AF skirt following procedures recommended by TDI, and as contained in Reference 3-2, was measured. Multiplying the measured strain by Young's modulus for steel and the area of the central portion of the stud provided a stud load, F_{B0} , of 6600 pounds.

A load-displacement measurement was performed on a stack of Belleville washers assembled according to instructions in Reference 3-2 for modified AF skirts (i.e., two stacks of 13 washers each placed concave end-to-concave end, with a central alignment bushing). The measurement was performed in a closed loop servohydraulic test machine, and the stiffness of the washer stack was found to be $k_w = 0.15$ kips/mil.

The spring constant of the stud, which is idealized as having a length equal to the length of its reduced section (3.765 inch) is equal to 2.52 kips/mil. Since the stud and washer stack are in parallel, their combined stiffness will be

$$k_{sw} = \left(\frac{1}{k_{stud}} + \frac{1}{k_w} \right)^{-1} = 0.142 \text{ kips/mil} \quad (\text{AF})$$

The stiffness of the washer stack for an AE piston is twice that of a modified AF, because a single stack of 13 washers is used for the AE. Therefore, $k_w = 0.30$ kips/mil, which results in a combined stud/washer stiffness of

$$k_{sw} = 0.268 \text{ kips/in} \quad (\text{AE})$$

These results are used in the crown/skirt interaction model.

3.2 Crown/Skirt Interaction Model

The finite element analyses reported in Reference 3-1 and summarized above provided information on stress levels in the piston assembly, and allowed estimates of gap closure pressures at ambient temperature. Additionally, the finite element results summarized in Figures 2-4 and 2-5 suggest that gap closure is uniform around the circumference of the skirt, which is consistent with experimental observations. However, information on the influence of thermal distortion on the load split between the loading rings and the possibility of lift-off of the crown from the skirt during the exhaust stroke was not provided directly by the finite element results. All of these additional factors could be incorporated into finite element models, but such a model would be a significant extension beyond those employed to date -- the primary extension being the use of gap elements in both loading rings. This would result in nonlinear effects which would require an iterative solution to an already large problem. The inclusion of thermal distortion effects would also produce additional complexities.

Rather than undertake additional expansions of a three-dimensional crown/skirt model, a simple engineering model that accounts for all of the important variables was constructed. The model was based on the observation that the gap appears to close uniformly around the circumference. This is consistent with both the experimental observations and finite element calculations.

The model was based on the assumption that the loading rings on the crown and the skirt remain parallel to one another. For the purpose of evaluating stiffnesses, the loading rings were assumed to remain planar. The stiffnesses and crown thermal distortion reported in Section 2.3 provide necessary inputs to the crown/skirt interaction model. Two basic conditions were considered; (i) top dead center of the compression stroke (or beginning of power stroke), where the maximum compressive stresses in the piston skirt

occur, and (ii) top dead center of the exhaust stroke, where lift-off of the crown may occur. Lift-off would alter the load path for the reaction of the stud preloads, and, as shown in Table 2-1, would result in increased maximum tensile stresses in the skirt.

3.2.1 Power Stroke

The maximum firing pressure of 1670 psig is considered to occur at top dead center of the compression stroke (which coincides with the beginning of the power stroke). Figure 3-1 shows the forces acting on the crown and skirt at this point (inertia forces are included as a reduction in the pressure). F_i is the total load on the inner ring, and F_o is the total load on the outer ring. Both of these loads are distributed around the circumference of their corresponding ring. F_o is obviously zero prior to closure of the gap, g_o . The stud preloads do not enter into the problem unless lift-off occurs, which is not possible under firing load conditions. The displacement of the inner and outer rings of the skirt are given by the following expressions:

$$\begin{aligned}\delta_i &= \frac{F_i}{k_{ii}} + \frac{F_o}{k_{io}} \\ \delta_o &= \frac{F_o}{k_{oo}} + \frac{F_i}{k_{oi}}\end{aligned}\tag{3-1}$$

where k_{oo} = stiffness of outer ring due to load at outer ring
 k_{io} = stiffness of outer ring due to load at inner ring
 k_{ii} = stiffness of inner ring due to load at inner ring
 k_{oi} = stiffness of inner ring due to load at outer ring

The reciprocal theorem of linear elasticity (page 240, Reference 3-3) requires that $k_{io} = k_{oi}$. The following relationships are employed to simplify the notation:

$$\begin{aligned}k_i &\equiv k_{ii} \\ k_o &\equiv k_{oo}\end{aligned}\tag{3-2}$$

Equation 3-1 then becomes

$$\begin{aligned}\delta_o &= \frac{F_o}{k_o} + \frac{F_i}{k_{oi}} \\ \delta_i &= \frac{F_i}{k_i} + \frac{F_o}{k_{oi}}\end{aligned}\tag{3-3}$$

Force equilibrium of the crown results in the following relationship

$$F_o + F_i = pA\tag{3-4}$$

where A is the cross-sectional area of the cylinder.

Let δ_c be the downward displacement of the outer ring of the crown relative to the inner ring of the crown. Pressure, p , produces a downward displacement, F_o produces an upward displacement and thermal distortion results in a downward displacement. The following relationship holds

$$\delta_c = \frac{pA}{k_{c(p)}} + \delta_T - \frac{F_o}{k_{c(F)}}\tag{3-5}$$

where $k_{c(p)}$ = stiffness of crown due to uniform pressure

$k_{c(F)}$ = stiffness of crown due to outer ring loading

δ_T = thermal distortion of crown, which is considered to be known (see Section 2.3.2).

The following expression follows from the geometrical relationship between the displacements

$$\delta_i - \delta_o + \delta_c = g_o - g\tag{3-6}$$

The current value of the gap is denoted by g , the initial value is g_o , and $g = 0$ when the gap is closed.

The following parameters are considered as unknowns: F_o , F_i , δ_o , δ_i , g , and δ_c . However, if $g \neq 0$ then $F_o = 0$, and vice versa. Therefore, there are five unknowns. The five equations necessary for a solution are given by Equations 3-3, 3-4, 3-5, and 3-6.

tions 3-3 (two equations), 3-4, 3-5, and 3-6. Under ambient conditions with no pressure, the gap is equal to its initial value, g_0 .

* The pressure at which the gap first closes at room temperature (hence $\delta_T = 0$) is of particular interest. This pressure is denoted as p^* and is given by the following expression ($\delta_T = g = F_0 = 0$)

$$p^* = \frac{g_0}{A \left[\frac{1}{k_{c(p)}} + \frac{1}{k_i} - \frac{1}{k_{i0}} \right]} = \frac{g_0}{pA \left[\frac{1}{k_{c(p)}} + \frac{1}{k'_i} \right]} \quad (3-7)$$

The notation $k'_i = [(1/k_i) - (1/k_{i0})]^{-1}$ has been introduced for simplicity.

The forces on the load rings once the gap has closed are of interest, because the load "split" influences the stresses. Taking $g = 0$ (because the gap has closed) and using the five simultaneous equations leads to the following expression for the force on the outer ring

$$F_0 = \frac{\delta_T - g_0 + pA \left[\frac{1}{k_{c(p)}} + \frac{1}{k_i} - \frac{1}{k_{i0}} \right]}{\frac{1}{k_{c(F)}} + \frac{1}{k_o} + \frac{1}{k_i} - \frac{2}{k_{oi}}} \quad (3-8)$$

$$= \frac{\delta_T - g_0 + pA \left[\frac{1}{k_{c(p)}} + \frac{1}{k'_i} \right]}{\frac{1}{k_{c(F)}} + \frac{1}{k'_i} + \frac{1}{k'_o}}$$

The notation $k'_o = [(1/k_o) - (1/k_{i0})]^{-1}$ has been introduced for simplicity and to facilitate comparison with experimental results.

The ratio of F_0 to F_i is useful in comparisons with experimental observations. Using Equation 3-4 to obtain an expression for F_i in terms of p and F_0 and dividing this into Equation 3-9 for F_0 provides the following result (for $p > p^*$):

$$\frac{F_o}{F_i} = \frac{pA\left[\frac{1}{k_{c(p)}} + \frac{1}{k_i'}\right] + \delta_T - g_o}{pA\left[\frac{1}{k_{c(F)}} - \frac{1}{k_{c(p)}} + \frac{1}{k_o'}\right] - \delta_T + g_o} \quad (3-9)$$

Gap closure pressure and load splits calculated by use of Equations 3-7 and 3-9 in conjunction with finite element stiffness values are compared with (room temperature) measurements in Section 3.3.

3.2.2 Exhaust Stroke

The analysis to determine whether the crown and skirt separate on the inner ring during the exhaust stroke follows procedures similar to those employed above. Whether or not such "lift-off" occurs has an important influence on the peak tensile stresses during the exhaust stroke. The crown is attached to the skirt by four studs, each of which has a static preload of F_{B0} , as discussed in Section 3.1.2. Figure 3-2 shows the forces acting on the crown and skirt, where now a separation of δ_L on the inner load ring is considered. The separation distance, δ_L , is taken to be independent of angular position, which is consistent with the assumption that the loading rings remain parallel to one another. This assumption underestimates the deformation of the skirt under actual stud loading conditions, because, as shown in Figure 2-1, deformation of the top of the crown is far from uniform under stud loading conditions. Additional possibilities are lift-off over part of the inner contact ring at a given angular location, or over a part of the circumference of the loading ring. Rotation of the inner crown ring relative to the inner skirt ring, resulting in stud bending, could also occur. The assumption of a uniform δ_L will lead to conservative predictions regarding lift-off, i.e., lift-off may be predicted under situations where it does not actually occur. Additional comments along these lines are provided in Section 4.1, where displacements based on the model are compared with the finite element results for stud loading.

Once a lift-off distance of δ_L is present, the force in a single stud is given by:

$$F_B = F_{Bo} + k_{sw} \delta_L \quad (3-10)$$

where k_{sw} is the stiffness of the stud/washer combination*.

For the purposes of estimating skirt deformation, assume the bolt loads to be distributed around the inner load circle. By use of Equation 3-3, the skirt distortion is given by the following expression:

$$\delta_s = 4F_B \left(\frac{1}{k_i} - \frac{1}{k_{oi}} \right) + F_o \left(\frac{1}{k_o} - \frac{1}{k_{oi}} \right) = 4 \frac{F_B}{k_i} + \frac{F_o}{k_o} \quad (3-11)$$

Force equilibrium of the crown provides the following relationship

$$4F_B = F_o + F_I \quad (3-12)$$

where F_I is the crown inertia force (see Figure 3-2). The distortion of the crown due to the force F_o is given by (see Equation 3-5)

$$\delta_{c(F)} = \frac{F_o}{k_{c(F)}} \quad (3-13)$$

Displacement compatibility provides the following relationship

$$\delta_L + \delta_s = \delta_T - g_o - \delta_{c(F)} \quad (3-14)$$

Recall that δ_L is positive upward, and δ_L will be decreased by a larger gap, a larger skirt distortion, and a larger upward outer crown ring displacement due to F_o . A larger thermal distortion (δ_T) will increase lift-off.

* The stud is assumed to be rigidly attached to the crown, and inner-ring crown distortion and "through thickness" skirt displacement are assumed to be negligible.

There are now five unknowns [F_B , δ_L , δ_s , F_0 , and $\delta_c(F)$]. Equations 3-10 through 3-14 provide the five equations necessary for a solution. This system of equations provides the following results:

$$\begin{aligned} \delta_L(1 + \omega) &= \delta_T - g_0 - \frac{\omega}{k_{sw}} F_{Bo} \\ &+ F_I \left[\frac{1}{k_{c(F)}} + \frac{1}{k_o} - \frac{1}{k_{oi}} \right] \end{aligned} \quad (3-15)$$

The constant ω is defined by the following:

$$\omega = 4k_{sw} \left[\frac{1}{k_{c(F)}} + \frac{1}{k_i} + \frac{1}{k_o} - \frac{2}{k_{oi}} \right] = 4k_{sw} \left[\frac{1}{k_{c(F)}} + \frac{1}{k_i} + \frac{1}{k_o} \right] \quad (3-16)$$

Once δ_L is known, the stud load is given directly by Equation 3-10, and the force F_0 is given by the following expression obtained by combining Equations 3-10 and 3-12.

$$F_0 = 4(F_{Bo} + k_{sw} \delta_L) - F_I \quad (3-17)$$

Positive values of δ_L and F_0 confirm that lift-off has occurred. If lift-off has not occurred, then the results of Section 3.2.1 must be used if it is desired to estimate F_i and F_0 (with an appropriate value of p to account for the inertia force).

For a given set of conditions, the minimum allowable gap to preclude lift-off (denoted as g_0^*) is obtainable from Equation 3-15 by setting $\delta_L = 0$. This provides the following expression

$$\begin{aligned} g_0^* &= \delta_T - \frac{\omega}{k_{sw}} F_{Bo} + F_I \left[\frac{1}{k_{c(F)}} + \frac{1}{k_o} - \frac{1}{k_{oi}} \right] \\ &= \delta_T - \frac{\omega}{k_{sw}} F_{Bo} + F_I \left[\frac{1}{k_{c(F)}} + \frac{1}{k_o} \right] \end{aligned} \quad (3-18)$$

Lift-off will occur if $g_0 < g_0^*$. Using the relationship for g_0^* given by Equation 3-18, Equation 3-15 can be rewritten as follows:

$$\delta_L = \frac{g_0^* - g_0}{1 + \omega} \quad (3-19)$$

• Comparison of gap closure pressures and load splits as observed experimentally and as predicted by the crown/skirt model are presented in the next section. The possibility of lift-off and the effects on cyclic stresses are discussed in Section 4.1 where cyclic stress magnitudes are estimated for piston skirts at ambient and steady-state operating temperature conditions.

3.3 Comparison with Experimental Observations

The gap closure pressure and load split between rings can be evaluated from the crown/skirt interaction model using the spring constants evaluated by finite elements. The gap closure pressure, p^* , can be evaluated by means of Equation 3-7. The ratio of peak stress with closure to the corresponding value in the absence of closure can be evaluated knowing the ratio of forces on the outer and inner rings, as given by Equation 3-9, assuming that the peak stress is governed by the load on the inner ring. The results of Table 2-1 show that this assumption is a good approximation, because the stresses for a given load that is applied by a uniform displacement on the inner ring are much higher than corresponding values for loading on the outer ring. The ratio of stresses with and without closure is given by the following expression:

$$\frac{\sigma_{\text{closure}}}{\sigma_{\text{(no closure)}}} = \frac{F_i}{F_o + F_i} = \frac{1}{1 + \frac{F_o}{F_i}} \quad (3-20)$$

The value of F_o/F_i is obtainable from Equation 3-9.

Table 3-2 summarizes the calculated gap closure pressure and stress ratio; the nominal, minimum and maximum values correspond to the gap values shown in Table 3-1. A comparison of Tables 3-1 and 3-2 reveals good agreement between the results predicted by the crown/skirt interaction model and the

experimental observations for the case of the AE piston. The load split prediction for the AF skirt is also good, and the gap closure pressures agree within about 20%.

The comparison between the experiments and calculations can also be made by estimating skirt stiffnesses from experimentally observed load splits and gap closure pressures and comparing the results with the finite element stiffnesses. Table 3-3 summarizes the results of such comparisons, which show better agreement for the AE than for the AF skirts. Experimental values of the outer skirt stiffness (k'_0) are generally lower than calculated. However, the finite element values fall within the range of results calculated by use of experimental observations.

Overall, the agreement between the various sets of data is quite good, which indicates the validity of the crown/skirt interaction model. Fortunately, as shown in the next section, the predicted cyclic stresses and crack growth are not highly dependent on the accuracy of the predicted skirt stiffnesses. The major value of the crown/skirt interaction model is its ability to predict cyclic stresses in a piston skirt at operating temperatures, which is discussed in the following section.

Section 3 References

- 3-1. "Investigation of Types AF and AE Piston Skirts," Report prepared by Failure Analysis Associates for Transamerica Delaval Inc. Diesel Generator Owners Group, Report No. FaAA-84-2-14, Palo Alto, California, May 1984.
- 3-2. Instructions for AF Piston Skirt Modification contained in letter from TDI to LILCO referenced as part of Stone and Webster Engineering Corporation Engineering and Design Coordination Report No. F-38313, December 3, 1981.
- 3-3. S.P. Timoshenko and J.N. Goodier, Theory of Elasticity, Second Edition, McGraw-Hill Book Company, Inc., New York, 1951.

Table 3-1
SUMMARY OF EXPERIMENTAL OBSERVATIONS
RELATED TO CROWN/SKIRT INTERACTION
(From Reference 3-1)

		AE	AF
Gap, g_0 , mils	nominal	7.5	8.0
	min	7.0	7.5
	max	8.0	9.5
Gap closure pressure, p^* , psig	nominal	1000	800
	min	820	700
	max	1050	1000
$\sigma_{\text{closure}}/\sigma_{\text{(no closure)}}$ at 1670 psig	nominal	0.88	0.80
	min	--	0.75
	max	--	0.92

Table 3-2
GAP CLOSURE PRESSURE AND STRESS REDUCTIONS
DUE TO GAP CLOSURE AS PREDICTED FROM CROWN/SKIRT MODEL

		AE	AF
Gap closure pressure, p^* , psig (Equation 3-7)	nominal	1040	1050
	min	970	980
	max	1110	1240
$\sigma_{\text{closure}}/\sigma_{\text{(no closure)}}$ at 1670 psig (Equations 3-9 and 3-20)	nominal	0.85	0.85
	min	0.83	0.83
	max	0.87	0.89

Table 3-3
COMPARISON OF SKIRT STIFFNESSES AS EVALUATED FROM EXPERIMENTAL OBSERVATION
AND CROWN/SKIRT INTERACTION MODEL WITH CORRESPONDING FINITE ELEMENT VALUES

			AF	AF	Comments
EXPERIMENTS	k'_1 , kips/mil	nominal	83.7	44.4	Evaluated by use of Equation 3-7, using $k_c(p) = 47.4$ kips/mil and various observed p^* and q_0 from Table 3-1.
		min	45.7	25.8	
		max	121	81.7	
	k'_{0*} , kips/mil	nominal	7.95	31.9	Evaluated by use of Equation 3-9 and 3-20 using k'_1 from above, $k_c(p) = 16.4$ kips/mil and various observed load splits and q_0 from Table 3-1.
		min	24.0	8.0	
		max	283	-	
FINITE ELEMENTS	k_1 k_{0*} k_{10}		81.2	70.5	From Table 2-2.
			95.3	94.2	
			500	500	
	k'_1 k'_{0*}		96.9	82.1	From k_1 , k_{0*} and k_{10}
			118	116	

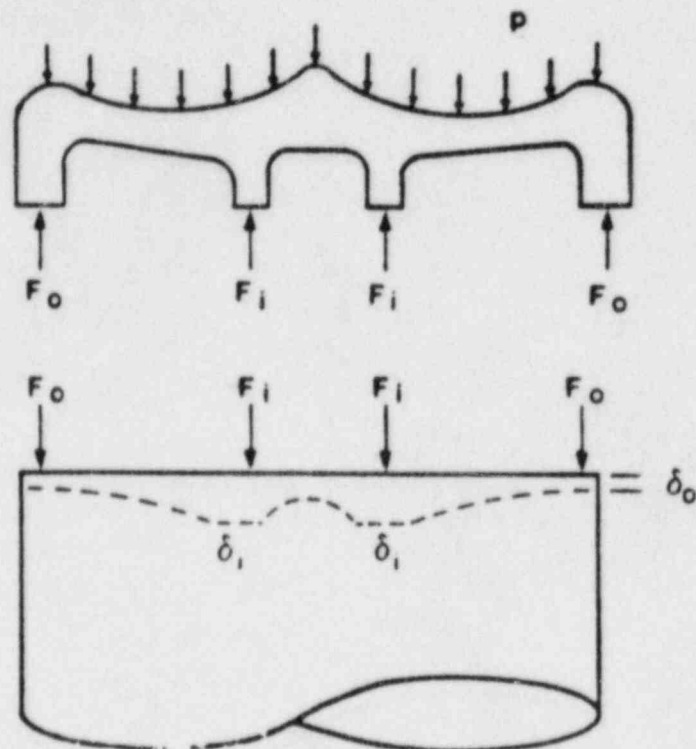


Figure 3-1. Schematic representation of loads and displacements on inner and outer contact rings of crown and skirt.

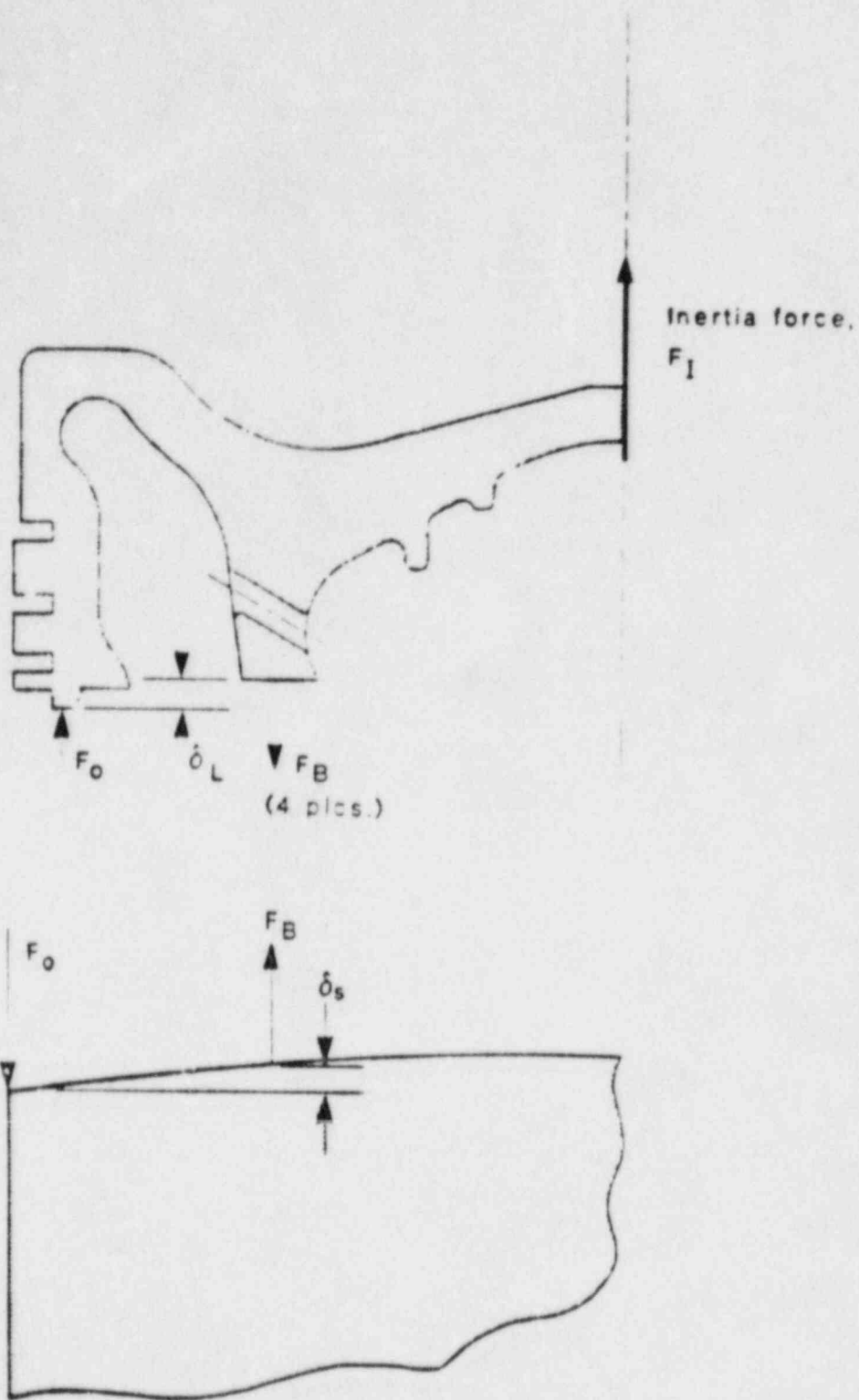


Figure 3-2. Forces acting on crown and skirt at
for dist center of exhaust stroke.

4.0 FATIGUE AND FRACTURE ANALYSIS

Previous work reported in Reference 4-1 included analyses of fatigue crack initiation, propagation, and arrest in AE and AF piston skirts under isothermal conditions. The cyclic stresses employed accounted for gap closure and load split in the AF piston by linear interpolation between results for the two gap sizes employed in the testing of the skirt. In this section, a similar analysis is performed, including the influence of thermal distortion of the crown. The crown/skirt interaction model is used to predict the load split in pistons with isothermal and steady-state operating temperature distributions, and these results are then used to adjust the stresses in the crown/skirt model to account for the load split and possible crown lift-off. Once the cyclic stresses have been calculated for various conditions, the possibility of crack initiation, growth and arrest is analyzed by fatigue and fracture mechanics procedures that are described in Reference 4-1.

4.1 Cyclic Stresses

The finite element stresses for the complete crown/skirt finite element model and for lift-off, as summarized in Table 2-1, form the basis for estimating the cyclic stresses in pistons with isothermal and steady-state temperature distributions and various initial gap sizes. These base line stresses are adjusted by use of the crown/skirt interaction model to account for thermal distortion, gap closure, and other operating variables. Reference 4-1 shows that the finite element results are generally conservative relative to experimental isothermal stresses. Hence, the following results are also conservative.

In order to encompass the load splits observed experimentally, cyclic stresses are evaluated using the range of skirt stiffnesses estimated from experimental observations. The skirt stiffnesses evaluated by finite element calculations are also considered. Hence, the four sets of k_f and k_o shown in Table 3-3 for each skirt design are considered. Table 4-1 provides a summary of the results. σ_{max} for an isothermal piston is always equal to σ_{max} for no lift-off. σ_{max} for a piston with steady-state temperature distribution

depends upon whether or not lift-off takes place. A value of $\delta_L = 0$ implies no lift-off.

The results of Table 4-1 show that the cyclic stress amplitude is lower in the case of steady-state temperature distribution than in the isothermal case even when lift-off is predicted to occur. Hence, isothermal operating conditions are generally more severe than steady-state conditions. A smaller gap always results in a more favorable q_{min} , but may produce a less favorable q_{max} because of the possibility of lift-off with a smaller gap. The results of Table 4-1 show that lift-off is almost always predicted for an initial gap of 0.007 inch, but never for a 0.011 inch gap.

A comparison of the predicted lift-off distances with predicted skirt displacements under stud loading is shown in Figures 4-1 and 4-2, which presents the results from Figure 2-1 along with corresponding predicted values of δ_i and δ_L for the two types of piston skirts. The values of δ_L are calculated using the skirt stiffnesses from finite element analysis. These figures show that the skirt deforms more under washer landing loads than is predicted by use of the spring constants for uniform inner ring displacement. This is not unexpected; the stiffness of the skirt under uniform displacement loading is dominated by the relatively very stiff region near the wrist pin. Figures 4-1 and 4-2 show that the skirt can deform sufficiently to preclude lift-off when a 0.009 inch initial gap is present. However, the calculated lift-off for a 0.007 inch gap is much larger than any skirt displacement due to stud loading. Therefore, it appears that lift-off is likely to occur with a 0.007 inch gap, but not for a 0.009 inch or larger gap. Also, the larger washer landing displacements for the AF means that this skirt can more closely follow the crown at top dead center of the exhaust stroke, and lift-off is, therefore, less likely than in the AE.

4.2 Fatigue Crack Initiation Analysis

The cyclic stresses in piston skirts with isothermal and steady-state temperature distributions presented in Table 4-1 are combined with the fatigue crack initiation criteria from Reference 4-1 to assess the possibility of cracks initiating in AE and AF piston skirts under a variety of conditions.

Figures 4-3 and 4-4 show the results for 0.007 and 0.011 inch initial gaps for isothermal and steady-state temperature distribution conditions. Two results are shown for each set of conditions, corresponding to the minimum and maximum values from Table 4-1. Allowable stress envelopes for maximum and minimum yield strength values from Table 2-2 of Reference 4-1 are indicated, which is the same procedure as employed in the earlier report.

Figures 4-3 and 4-4 show that conditions for crack initiation are more severe under isothermal conditions and with a large gap. Even though lift-off is predicted for steady-state operation with a 0.007 inch gap, the resulting cyclic stresses are less likely to initiate cracking than with a 0.011 inch gap which does not experience lift-off. Figure 4-3 shows that cracks might initiate in AE skirts under certain conditions. In contrast, Figure 4-4 shows that cracks are predicted to initiate in the AF skirt under isothermal conditions for any gap size considered, and initiation might occur under cyclic stresses corresponding to steady-state operation. These observations are consistent with those reported in Reference 4-1 for isothermal conditions. Although fatigue cracks may initiate in the piston skirts, these cracks will not necessarily propagate, because they would grow into a region of decreasing stresses.

4.3 Fatigue Crack Growth Analysis

The results of the previous section reveal that cracks may initiate in the stud boss region of AE and AF piston skirts. This section analyzes the cracks to determine if they will grow, and if so, whether they will subsequently arrest. Arrest is likely to occur because of the very steep stress gradient in the stud boss region (see Figure 4-1 of Reference 4-1). Fatigue crack growth analyses were performed for the cyclic stress conditions included in Table 4-1 by procedures described in Reference 4-1. The normalized stress gradient in all cases was taken to be the same as that shown in Figure 4-1 of Reference 4-1. The only modification to earlier procedures was to consider a combination of stresses corresponding to isothermal and steady-state conditions. Calculations were first performed for cyclic stresses under isothermal conditions. Possible stress redistribution due to yielding was considered.

Fatigue crack growth due to the redistributed stresses was analyzed. This was followed by imposition of stresses corresponding to steady-state operation. In some instances, cracks could grow deeper under steady-state conditions than isothermal, because σ_{max} increases if lift-off occurs. Following procedures in Reference 4-1, two sets of calculations were performed, one for nominal tensile properties and one for worst-case tensile properties.

Cracks were predicted not to propagate in the AE skirt under any condition considered. In contrast to this, cracks were predicted to grow in the AF skirt in certain cases, but always to arrest. Table 4-2 summarizes the crack growth and arrest results. In contrast to the results presented in Reference 4-1, cracks were predicted to grow in AF pistons with gaps within the TDi-specified range of 0.007 - 0.011 inch on assembly. The cyclic stresses as a function of gap were evaluated in Reference 4-1 by a procedure that differed from the crown/skirt interaction model employed here. This resulted in different values of the estimated cyclic stresses.

Table 4-2 shows that, if cracks are predicted to propagate at all, they will arrest at depths ranging from 0.10 to 0.49 inch. The predicted depth of arrested cracks is larger than in Reference 4-1 because of the different means of estimating cyclic stresses and the consideration of lift-off between the skirt and the crown. Observed crack depths reported in Reference 4-1 were in the range of 0.10 to 0.30 inch. The values in Table 4-2 with and without lift-off bracket this observed range. As discussed earlier, the crown/skirt interaction model tends to overpredict lift-off, which would lead to overpredicting σ_{max} . This, in turn, would overpredict the arrested crack depth.

Overall, cracks are always predicted either not to grow or to arrest at depths comparable to observed values. Hence, the earlier conclusions [4-1] regarding the integrity of the AE and AF skirts under isothermal conditions are also applicable to steady-state operation.

Section 4 References

- 4-1 "Investigation of Types AF and AE Piston Skirts," Report prepared by Failure Analysis Associates for Transamerica Delaval Inc. Diesel Generator Owners Group, Report No. FaAA-84-2-14, Palo Alto, California, May 1984.

Table 4-1
CYCLIC STRESSES IN AE AND AF PISTON SKIRTS UNDER
ISOTHERMAL AND STEADY-STATE CONDITIONS

Notes		AE				AF			
		F.I.	nominal	min	max	F.I.	nominal	min	max
σ_{\min}	1	<----- -68.1 ----->				<----- -92.2 ----->			
σ_{\max} lift-off	1	<----- 7.32 ----->				<----- 17.8 ----->			
no lift-off	1	<----- 1.77 ----->				<----- 2.40 ----->			
k_i^*	2	96.9	81.7	45.7	121	82.1	44.4	25.8	81.7
k_o^*	2	118	28.0	7.95	203	116	31.9	8.0	-
δ_1	q_o								
	7	1.999	1.403	0	2.140	2.027	1.378	0	2.179
	9	0.157	0	0	0.295	0.116	0	0	0.258
	11	0	0	0	0	0	0	0	0
σ_{\min} isothermal	4	-57.5	-59.7	-60.3	-58.4	-76.0	-77.4	-75.4	-74.4
	9	-62.1	-67.9	-67.0	-63.4	-82.2	-76.7	-77.6	-81.2
	11	-66.7	-66.2	-63.8	-68.1	-88.3	-81.2	-79.9	-88.1
σ_{\min} steady-state	5	-31.0	-42.7	-50.9	-31.5	-43.7	-49.4	-63.6	-37.5
	9	-37.6	-45.9	-52.7	-36.6	-49.8	-53.7	-65.9	-44.9
	11	-42.7	-49.1	-54.4	-41.6	-55.9	-58.0	-68.1	-51.8
σ_{\max} steady-state	6	7.91	7.74	1.77	7.96	18.6	18.3	2.40	18.6
	9	7.77	1.77	1.77	7.40	17.8	2.40	2.40	17.9
	11	1.77	1.77	1.77	1.77	2.40	2.40	2.40	2.40

all stresses in ksi, q_o and δ_1 in mils

Notes:

1. From Table 2-1.
2. From Table 3-1.
3. From Equation 3-15.
4. From Equations 3-20 and 3-9 with $\delta_1 = 0$.
5. From Equations 3-20 and 3-9 with $\delta_1 = 10.6$ mils.
6. Equals σ_{\max} with no lift-off if $\delta_1 = 0$, adjusted from finite element σ_{\max} with lift-off if $\delta_1 > 0$ by using Equation 3-10 to determine stud boss load and ratioing by F_R/F_{R0} to account for increased stud load over the value used for finite element calculations.

Table 4-2
VALUES OF THRESHOLD AND ARRESTED CRACK DEPTHS IN AF
PISTON SHAFT UNDER A VARIETY OF CONDITIONS
(all crack sizes in inches)

Stress Condition from Table 4-1		F _u F _t		nominal		min		max	
Tensile	$\sigma_{0.2}$ mills	a_{th}	a_{ar}	a_{th}	a_{ar}	a_{th}	a_{ar}	a_{th}	a_{ar}
nominal	7	*	*	*	*	*	*	*	*
	9	*	*	*	*	*	*	*	*
	11	*	*	*	*	*	*	*	*
worst	7	*	*	*	*	*	*	*	*
	9	*	*	*	*	*	*	*	*
	11	0.040	0.123	*	*	*	*	0.040	0.123
nominal	7	0.018	0.452	0.020	0.452	*	*	0.018	0.452
	9	0.018	0.452	*	*	*	*	0.018	0.452
	11	*	*	*	*	*	*	*	*
worst	7	0.021	0.494	0.022	0.494	*	*	0.021	0.494
	9	0.020	0.494	*	*	*	*	0.020	0.494
	11	0.043	0.104	*	*	*	*	0.043	0.104

NO LIFT-OFF

POSSIBLE LIFT-OFF

* Crack growth predicted to not occur.

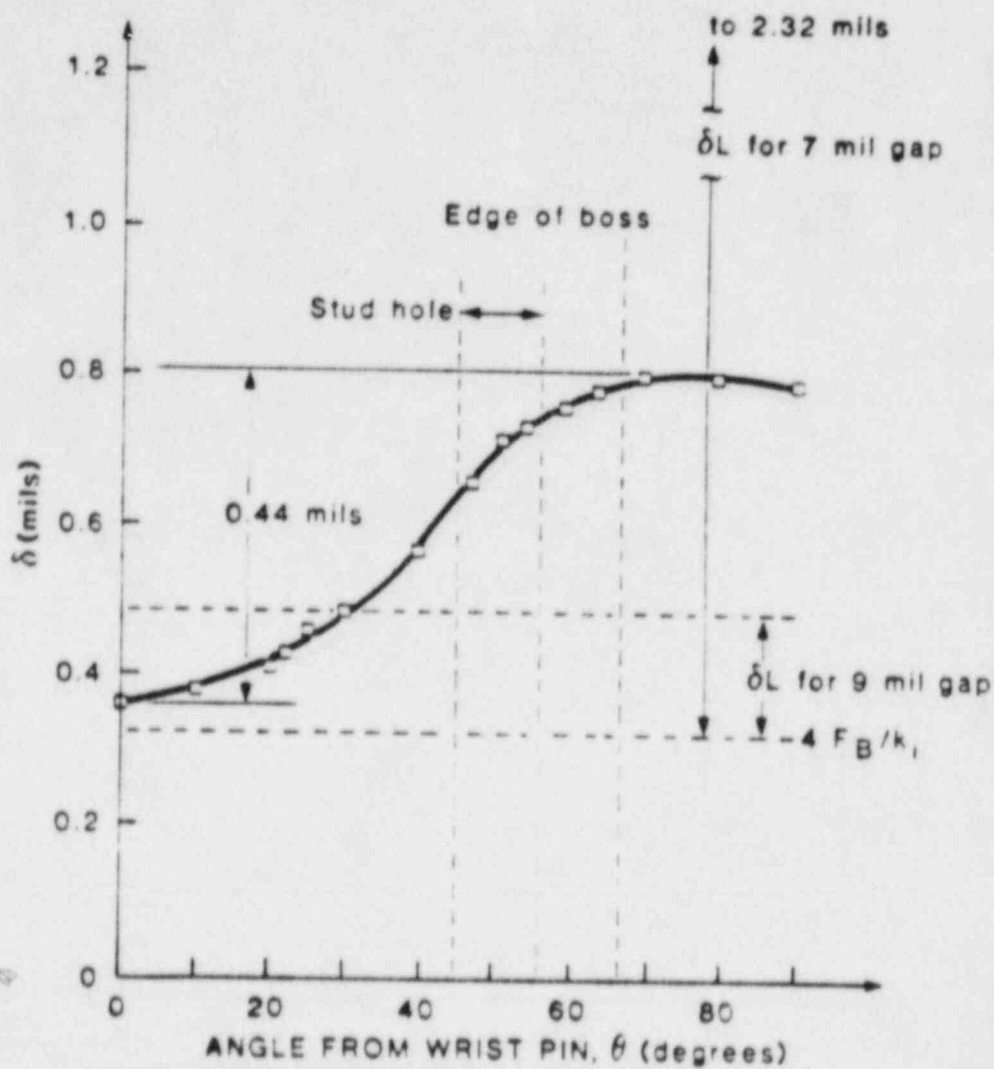


Figure 4-1. Lift-off distances compares with inner ring skirt displacements due to washer loads for the AE piston skirt.

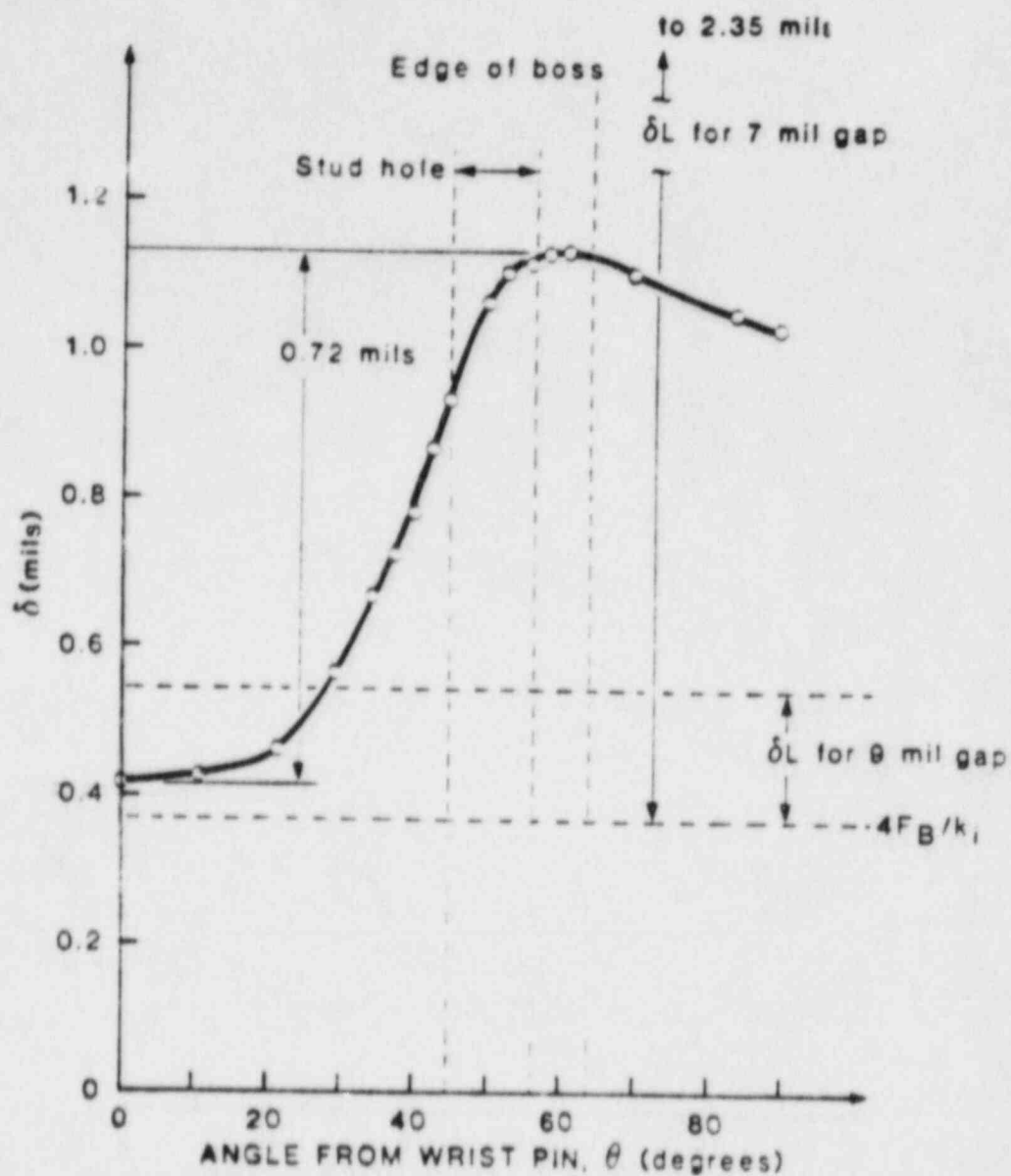


Figure 4-2. Lift-off distances compared with inner ring skirt displacements due to washer loads for the AF piston skirt.

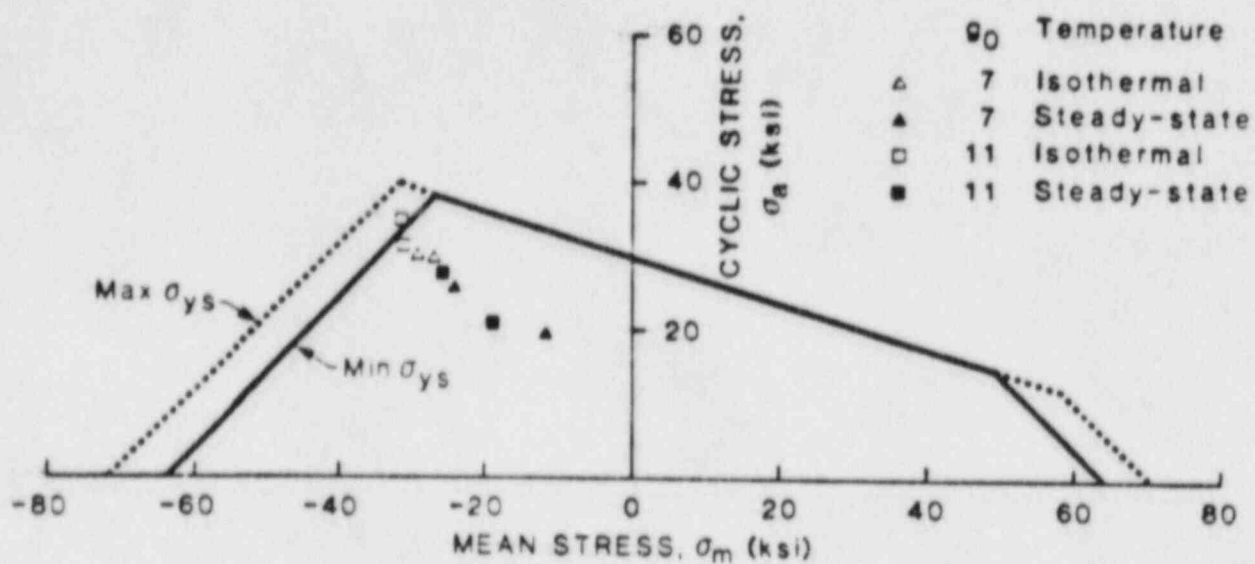


Figure 4-3. Stress states for Al primer skirt for various conditions plotted on graph of allowable stress amplitude as a function of mean stress.

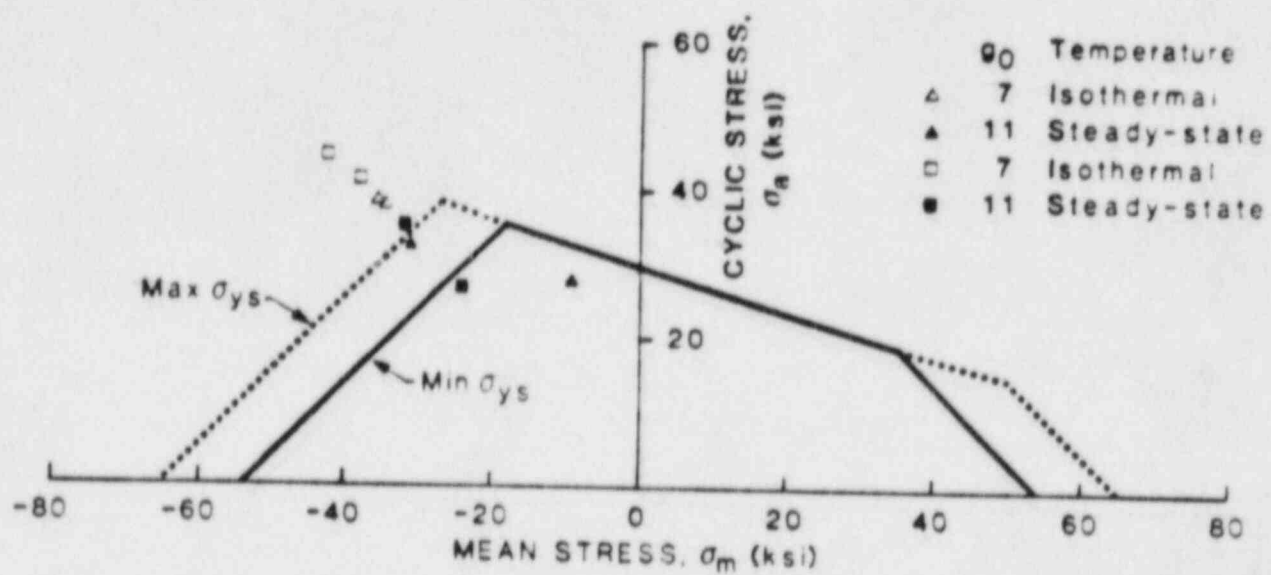


Figure 4-2. Stress states for AF piston skirt for various conditions plotted on graph of allowable stress amplitude as a function of mean stress.

5.0 CONCLUSIONS

A crown/skirt interaction model was developed that provides estimates of the influence of thermal distortion of the crown on cyclic stress levels in the stud boss regions of AE and AF piston skirts. This model extends results beyond those previously reported, which considered only isothermal conditions. The crown/skirt interaction model utilizes crown and skirt stiffnesses evaluated by finite element calculations. Comparisons with experimental observations showed generally good agreement with the model. Lift-off of the crown from the skirt was predicted for gap sizes less than about 0.009 inch at steady-state operating temperature. This lift-off alters the cyclic stresses.

Calculations of cyclic stresses under isothermal and steady-state operation were made using a range of stiffnesses encompassing experimental observations. Lift-off was considered in cases where it was predicted to occur. Crack initiation and propagation analyses were performed by procedures followed in earlier isothermal analyses. The conclusions obtained earlier regarding cracking of the AE and AF skirts were unchanged, but now the arrested crack depths predicted for the AF are in better agreement with field observations. Overall, the earlier conclusions regarding the integrity of the AE and AF skirts are also unchanged. These conclusions are that cracks may initiate but will not propagate in the AE, and that cracks will initiate and may propagate in the AF. However, any cracks in the AF are predicted to arrest at depths less than 0.5 inch, which is comparable to field observations.

APPENDIX A
Component Task Description

DR-03-341A-1

PISTONS
PART NO. 03-341A

Classification A
Completion 03/05/84

PRIMARY FUNCTION: The pistons react to the cylinder firing pressure and provide a reciprocating mechanism for converting combined inertia and combustion pressure forces into mechanical torque through the wrist pin, connecting rod, and crankshaft.

FUNCTIONAL ATTRIBUTES:

1. The piston crown must have sufficient strength to resist the high temperature and pressure firing loads.
2. The load transfer between the piston crown and skirt structure must not produce alternating stresses sufficient to cause failure of the skirt.
3. The wall structure of the skirt must be resistant to pressure-induced deformation which could result in skirt fatigue in proximity to the stiffening ribs.
4. Preload in the crown studs must be sufficient to preclude failures of studs/nuts/washers.
5. The piston skirt must provide a suitable sliding surface against the cylinder liner.
6. The piston ring groove must be sufficiently wear-resistant to provide sufficient ring life.

SPECIFIED STANDARDS: None

EVALUATION:

1. Determine the historical evolution of the AF, AF-modified, AH, AN, and AE piston designs, including casting, heat treatment, dimensional, and material changes.
2. Determine maximum firing pressures and temperatures for DSR-48, DSRV-16-4, DSRV-12-4, and DSRV-20-4 designs.
3. Develop finite element models for AF-modified and AE piston designs with pressure loading (static conditions).
4. Conduct thermo/mechanical analysis to determine thermally-induced load transfer due to crown distortion.
5. Perform metallurgical examination of fracture AF piston skirts.

6. Perform eddy current examination of AE piston skirts from TDI DSR-42 and R-5 engines, and Alaska stationary diesel generator.
7. Conduct fracture mechanics analysis of possible crack propagation in AF-modified and AE designs with differing stress conditions.
8. Conduct experimental static isothermal stress distribution test on AE skirt.
9. Evaluate the effect of piston skirt loading on wear.
10. Perform LP and eddy current inspection of SNPS AE pistons following 100 hours at 100% load.
11. Assess the similarity of the AF-modified, AH, and AN piston designs.
12. Complete report on AF-modified, AH, AN, and AE pistons.
13. Review information provided on TER's Q-159, Q-194, Q-203, Q-310, Q-326, Q-335, Q-338, Q-393, Q-412, Q-413, Q-419, and Q-422.

REVIEW TDI ANALYSES:

1. Examine TDI strain gage testing (static) on skirt stud boss region.

INFORMATION REQUIRED:

1. TDI drawings for AN and AE designs including studs, Belleville washers, preload, and material specifications.
2. Historical information on casting changes, heat treatment changes.
3. Maximum cylinder firing pressure and temperature for DSR-48, DSRV-16-4, DSRV-12-4, and DSRV-20-4.